Redox-responsive MRI Probes Based on First-row Transition Metal Complexes

Janet R. Morrow,* Jaclyn J. Raymond, Md Saiful I. Chowdhury and Priya Ranjan Sahoo

Department of Chemistry, University at Buffalo, the State University of New York, Amherst, NY
14260, United States.

Abstract

The presence of multiple oxidation and spin-states of first-row transition metal complexes facilitates the development of switchable MRI probes. Redox-responsive probes capitalize on a change in magnetic properties of the different oxidation states of the paramagnetic metal ion center upon exposure to biological oxidants and reductants. Transition metal complexes that are useful for MRI can be categorized according to whether they accelerate water proton relaxation (T_1 or T_2 agents), induce paramagnetic shifts of ^1H or ^{19}F resonances (paraSHIFT agents), or are chemical exchange saturation transfer (CEST) agents. The various oxidation state couples and their properties as MRI probes are summarized with a focus on Co(II)/Co(III) or Fe(II)/Fe(III) complexes as small molecules or as liposomal agents. Solution studies of these MRI probes are reviewed with an emphasis on redox changes upon treatment with oxidants or with enzymes that are physiologically important in inflammation and disease. Finally, we outline the challenges of developing these probes further for in vivo MRI applications.

I. Introduction

Magnetic Resonance Imaging (MRI) Contrast agents are paramagnetic metal complexes that are administered to enhance the images produced in diagnostic procedures.¹⁻⁴ Contrast agents modulate the proton resonances of water in soft tissue and are used to image blood flow, characterize tumors and lesions, and map heart function for augmenting the high-resolution images that characterize MRI.⁵ However, interest in determining disease prognosis and monitoring therapeutic response has given rise to a demand for a newer type of contrast agent which is called a molecular or responsive magnetic resonance imaging agent.^{6, 7} These agents produce signals in response to biological environment including changes in pH, redox status, metal ion concentrations, or protein targets.^{8, 9} Such molecular agents (or probes) are challenging to produce, but present a great opportunity for synthetic inorganic chemists.

The development of paramagnetic first-row transition metal complexes as MRI probes or contrast agents is based on a strategy to employ metal ions that are naturally present in the body. One goal is to prepare transition metal complexes that may serve as alternatives to the clinically-important Gd(III) based contrast agents. In addition to the advantage of being

essential elements that are also earth abundant, transition metal complexes have certain advantages in the development of responsive probes. One of the most obvious is the existence of multiple stable metal-based oxidation and spin states, something which is lacking for Gd(III) complexes. ^{10, 14} The ability to switch between oxidation and corresponding spin states in response to redox-related changes in biological environment is a powerful tool for molecular imaging. ^{8, 15, 16} For example, diseases such as cancer, stroke, and atherosclerosis are characterized by chronic inflammation which involves a perturbed biological redox environment. ^{17, 18, 19}

In this viewpoint, we focus on the coordination chemistry of first-row transition metal complexes and their use as redox-responsive probes with an emphasis on iron and cobalt complexes that undergo oxidation state changes at the metal center. We demonstrate the richness of the coordination chemistry of mononuclear and multinuclear complexes for tuning oxidation state and highlight current developments. We present several types of MRI probes including those that affect water proton relaxation, proton shift, and chemical exchange saturation transfer (CEST).^{1, 14, 20, 21} Transition metal coordination complexes as small molecule probes and as complexes loaded into liposomes will be discussed. This viewpoint is not meant to be a comprehensive review of first-row transition metal MRI probes which have recently been reviewed, ¹⁰ but rather to summarize approaches to redox-responsive transition metal MRI probes ^{16, 22} and to highlight the many challenges that remain in this budding area of research.

II. Categorization of first-row transition metal MRI probes

| Table 1. Common oxidation and spin states of transition metal-based MRI probes | | | | |
|--|--|--|---|--|
| | Mn(II) high-spin (T ₁ agent) | Mn(III) high-spin $(T_1 \text{ agent})$ | | |
| Fe(II) low-spin (diamagnetic) | Fe(II) high-spin (paraSHIFT/paraCEST) | Fe(III) high-spin $(T_1 \text{ agent})$ | Fe(III) low- spin (paraCEST) | Fe(II)-Fe(III) magnetically coupled (paraCEST) |
| | Co(II)-Co(II) high-spin (paraCEST) | Co(II) high-spin (paraSHIFT/paraCEST) | Co(III) low- spin (diamagnetic) | |
| | Ni(II) high-spin (paraCEST/paraSHIFT) | Ni(II) low-spin (diamagnetic) | | |
| | Cu(I) (diamagnetic) | Cu(II) (T ₁ agent) | Cu(II)-Cu(II) magnetically coupled (paraCEST) | |

Shown in Table 1 are several first-row transition metal ions in common oxidation and spin states that are used for MRI probe development. Given in parentheses is the MRI probe category that is commonly found in the literature for the spin and oxidation state shown in the table. MRI probes can be divided into two broad categories. 1, 3, 20 Metal complexes that promote the relaxation of water protons through either longitudinal (T_1) or transverse (T_2) relaxation processes are known as relaxation agents. Metal complexes that produce large paramagnetically-induced (hyperfine) shifts in the nuclear magnetic resonances of the probe ligand or surrounding water yet produce only moderate resonance broadening are known as shift agents. The key electronic properties of the paramagnetic complex which determine the MRI probe behavior are the number of unpaired electrons, their distribution in orbitals, and their electronic relaxation times.²³ Metal ions with electronic relaxation times on the order of the proton Larmor frequency of 10⁻⁸ to 10⁻⁹ s such as Mn(II), Fe(III), or Gd(III) are relaxation probes, whereas metal ions with shorter electronic relaxation times (<10⁻¹² s) such as Co(II) or Fe(II) are typically shift agents.²⁴ It is important to emphasize that the geometry of the metal center may have a large effect on magnetic properties of transition metal ions which may change the MRI probe category. Moreover, if there are multiple metal ion centers, magnetic coupling interactions may modulate spin and electronic relaxation properties as discussed in the examples below and shown in Table 1.

Relaxivity agents shorten the T_1 and T_2 proton relaxation times of water.^{3, 25} Notably, T_2 is always shortened more than T_1 ; common T_1 agents feature T_1/T_2 ratios that are typically about a factor of two or less. Contrast agents that are used clinically are T_1 agents that contain Gd(III) with polydentate or macrocyclic ligands.²⁶ Administration of the contrast agent produces positive contrast in the tissue where the contrast agents localize and are mapped through T_1 -weighted imaging. The T_1 agents are characterized by their relaxivity, T_1 , which is obtained from a plot of the proton relaxation rate constant as a function of contrast agent concentration and has the units of mM⁻¹s⁻¹.

$$r_1 = r_{1|S} + r_{1|S} + r_{1|OS}$$
 Eq. 1

Paramagnetic metal centers promote the relaxation of protons and other neighboring nuclei largely through dipolar interactions of unpaired electrons and nuclei. The water molecules that undergo proton relaxation may bind directly to the metal center (inner-sphere, r_{1IS}), indirectly through the coordination sphere (second-sphere, r_{1SS}) or through closely diffusing waters (outer-sphere, r_{1OS}). There are many studies of Gd(III) and Mn(II) complexes that have focused on optimizing inner-sphere interactions such as water exchange. By contrast, many studies of six-coordinate Fe(III) complexes have focused on second-sphere

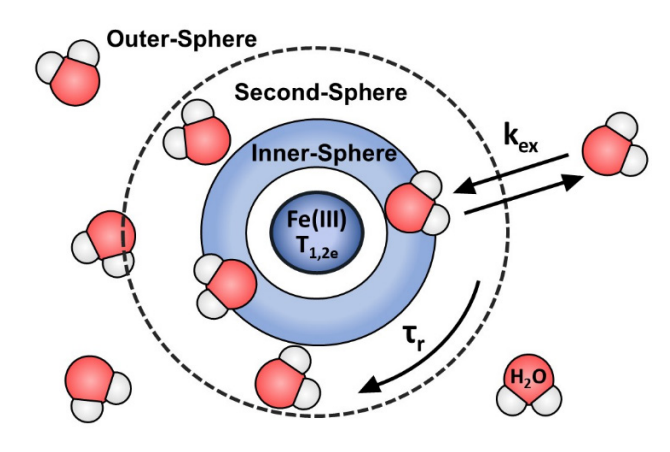


Figure 1. Parameters important for water proton relaxivity in high spin Fe(III) complexes

interactions given the slow rates of water exchange for these complexes. However, several seven-coordinate Fe(III) complexes have an exchangeable inner-sphere water. Relaxivity increases with the total electron spin quantum number of the complex, which at S = 5/2 for Mn(II) or Fe(III) is less than that of Gd(III) at S = 7/2. Relaxivity is dependent on magnetic field strength and temperature, so comparisons should be made at comparable field strengths and temperatures, and preferably at those most commonly used in human scanners (1.5 T or 3T) and at 37 °C.4

As shown in Figure 1, inner-sphere contributions to relaxivity depend on the rate constant for exchange of water (k_{ex}), the tumbling of the complex (rotational correlation time, (τ_r) and the electronic relaxation time (T_{1e}).² Water exchange rate constants and the number of inner-sphere waters are varied by strategic ligand design. Rotational correlation times can be modulated by increasing molecular weight through adding rigid linkers between metal centers, or by inducing binding to proteins and detailed analyses are reported for Gd(III) and Mn(II) complexes.^{13, 25, 30} Much less work has been reported to date for Fe(III) complexes on optimizing these parameters.¹² It has been noted that electronic relaxation times may limit the relaxivity of Fe(III) complexes at low magnetic field strengths. There remains much to learn about the role of the coordination sphere including donor groups and geometry for optimizing the relaxivity of Fe(III) contrast agents.^{11, 12}

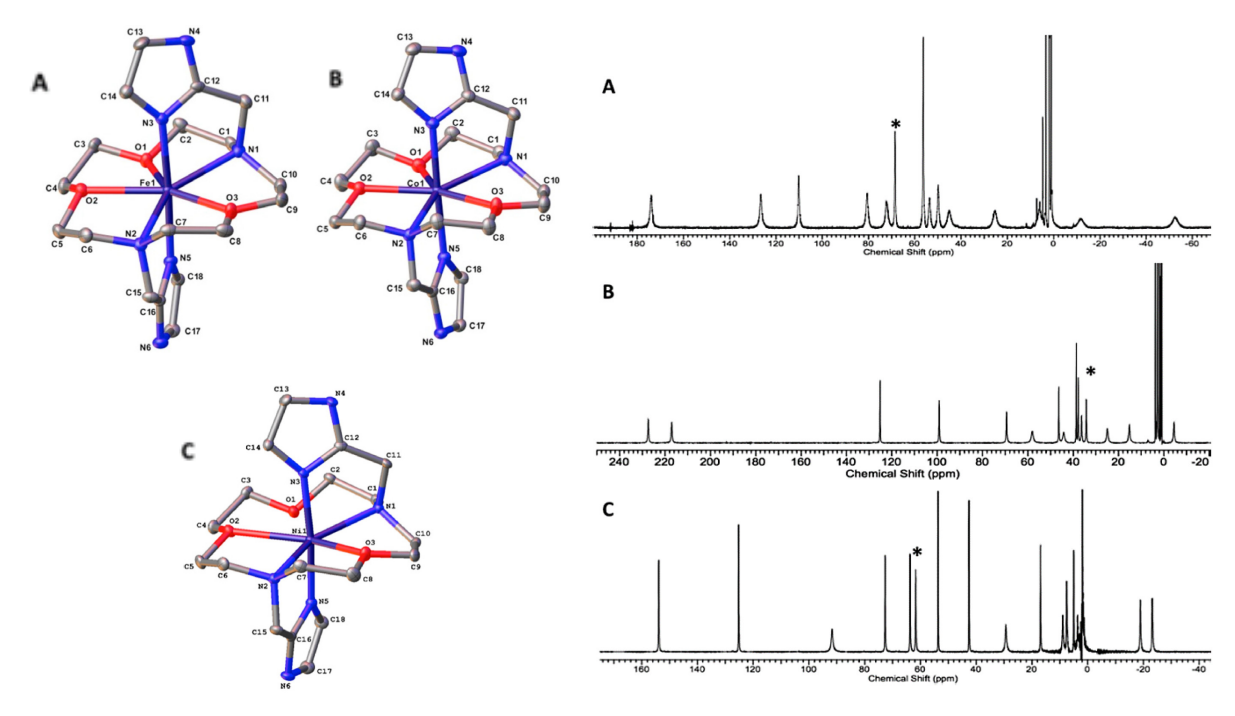


Figure 2. Proton NMR spectra of [Fe(HINO)]²⁺ (A) and [Co(HINO)]²⁺ (B) and [Ni(HINO)]²⁺ (C) in d₃-acetonitrile. Asterisk marks the exchangeable imidazole proton. Structure of the complex cations. HINO is N,N'-bis(imidazole-2-ylmethyl)-4,10-diaza-15-crown-5. Reprinted from ref. 30 with permission. Copyright 2017 American Chemical Society.

Metal ion complexes that are shift agents, such as high-spin Co(II), Fe(II), or Ni(II) complexes, show relatively sharp but highly dispersed proton resonances (Figure 2). In this case, the Co(II) complex shows sharper proton resonances than the Fe(II) complex in part due to oxidization of the complex to high-spin Fe(III) over time, which results in broadening of the resonances due to the enhanced proton relaxation promoted by the Fe(III) center. The chemical shift change from that of the free ligand is attributed to diamagnetic and paramagnetic contributions with paramagnetic or hyperfine contributions dominating these shifts (eq. 2). The hyperfine shift is produced by a combination of dipolar (δ_d , through space) and contact (δ_c , through bond) contributions with a smaller contribution from the diamagnetic shift (δ_d). For lanthanide complexes that lack substantial covalency in bonds, the hyperfine shifts are largely dipolar in nature for nuclei that are not directly bound to the metal ion. Pyperfine shifted resonances as shown by theoretical calculations.

$$\delta = \delta_d + \delta_c + \delta_p$$
 Eq. 2

There are several classes of MRI probe that contain a paramagnetic shift agent. For example, transition metal paraSHIFT agents show highly shifted ligand proton resonances that are temperature and pH dependent.³⁴⁻³⁷ When proton resonances of the ligands are monitored, the procedure is a Magnetic Resonance Spectroscopy (MRS) technique as compared

to measuring the proton resonance of water as in MRI.³⁸ Alternatively, paraSHIFT agents may contain fluorinated ligands for studies using ¹⁹F NMR spectroscopy. Various paramagnetic metal ions are used to shift the ¹⁹F resonance and to modulate the relaxation times of the ¹⁹F nuclei.²³ The paramagnetic shift can be modulated by changes in pH, temperature, and spin state as shown for Fe(II), Co(II) and Ni(II).^{33, 39, 40-42} Finally, if the metal complex produces hyperfine shifted protons of water ligands or of exchangeable protons on NH or OH groups of ligands, then a MRI probe based on paramagnetic chemical exchange saturation transfer (paraCEST) is created.^{21, 43} Transition metal paraCEST agents have an OH or NH proton that can chemically exchange with water protons.^{14, 44}

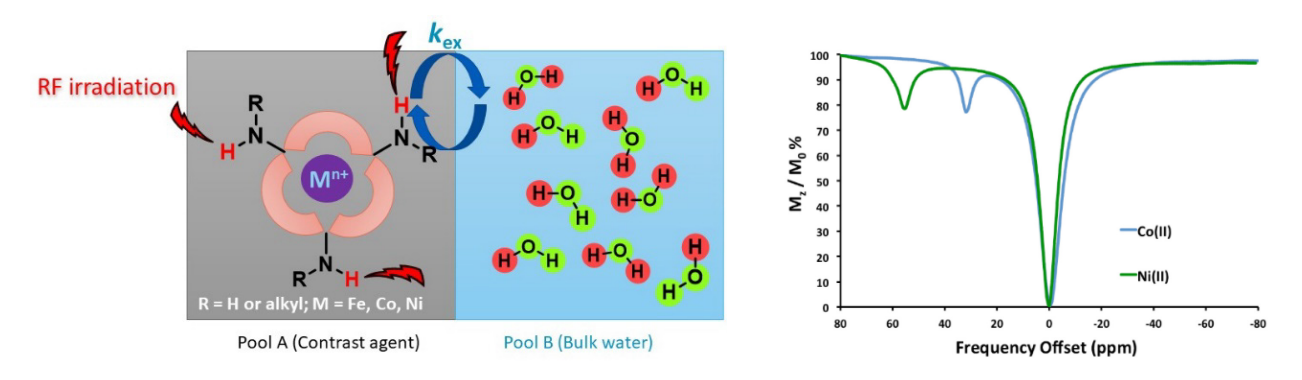


Figure 3. Left: schematic of CEST. Right: Z spectrum recorded at 11.7 T of 8 mM [Co(**HINO**)]²⁺ (blue) or [Ni(**HINO**)]²⁺ (green), in solution containing 100 mM NaCl, 20 mM HEPES, pH 7.0. Radiofrequency pulse of 4s applied at 37 °C, $B_1 = 24 \mu T$. Z spectrum reprinted from ref. 30 with permission. Copyright 2017 American Chemical Society.

In the CEST experiment, a presaturation pulse at the frequency of the exchangeable proton (NH or OH) magnetically saturates the proton. Exchange of the magnetically saturated ligand proton with water protons gives a reduction in the water proton signal. A plot of the normalized water signal intensity (M_z/M_0) against frequency offset (ppm) gives the Z-spectrum.^{21, 43} The paramagnetic center serves to shift the ligand proton resonances far away from the bulk water and the broad resonance from the magnetization transfer of protons in solid tissue (Figure 3). A CEST probe can be turned on or off based on the frequency and power of the radiofrequency pulse. A CEST phantom image on the MRI scanner is acquired by using a presaturation pulse either on-resonance or off-resonance of the exchangeable protons. The ratio between these two images is subtracted from 100% to give the CEST image as shown in Figure 7 for the Co(II) paraCEST agent described below.

CEST agents have the advantage of being "multicolor". In other words, each paraCEST agent may produce a CEST peak at a distinct frequency so that multiple CEST agents can be monitored and distinguished simultaneously. CEST agents are extremely sensitive to pH, which is attributed to acid- or base-catalyzed proton exchange. The shift of the exchangeable proton and the corresponding CEST peak are temperature dependent. One drawback of transition metal ion paraCEST agents is that even in simple solution (phantoms), low millimolar concentrations are required. This concentration is at least 10-fold higher than

that for T_1 agents.^{44, 48} Under conditions in vivo, the heterogeneity of environments coupled with the extreme sensitivity to environment makes it challenging to obtain contrast.⁴⁹ One way to increase sensitivity is to add the paraCEST agents to supramolecular structures such as silica nanoparticles⁵⁰ or liposomes.⁵¹ Another variation of CEST involves a fluorinated chelate that binds weakly to a metal shift agent, such as Fe(II). If the rate of exchange is optimized, a CEST signal can be generated based on the ¹⁹F resonance intensity.⁵²

Paramagnetic shift agents loaded into liposomes, which are vesicles with lipid bilayers, interact with the water molecules in the interior of the liposome to shift their resonances away from those of bulk water (Figure 4).⁵¹ If the liposome constituents are chosen to optimize water exchange between intraliposomal and bulk water pools, irradiation at the frequency of the intraliposomal water protons produces a CEST peak.⁵¹ Such agents are called "lipoCEST" probes. These experiments were elegantly pioneered for lanthanide shift agents,⁵³ and have recently been carried out with Co(II) agents.⁵⁴ Amphiphilic Co(II) complexes embedded in the bilayer lead to an additional contribution to the shift of the interior water protons. Finally, shrinking of the liposome to give oblong-shaped liposomes produces even larger intraliposomal water proton shifts through the addition of a bulk magnetic susceptibility contribution.⁵⁵ The advantage of lipoCEST is that the probes can be used in nanomolar concentrations. A disadvantage is that the CEST peak is much less shifted than that of typical paraCEST agents. Further, disruption of the liposome structure in the biological environment leads to destruction of the CEST signal.⁵⁶

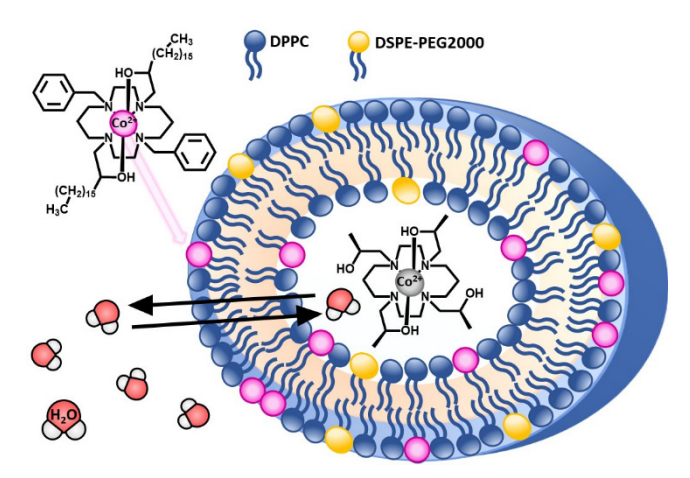


Figure 4. Co(II)-based liposomal CEST agents containing intraliposomal and amphiphilic complexes. Adapted with permission from ref. 53. Copyright 2020 Wiley

Liposomes loaded with paramagnetic relaxivity agents shorten water proton T_1 or T_2 relaxation times. To resumple, liposomes with Fe(III) or Mn(II) relaxivity agents incorporated into the bilayer are effective T_1 agents, as the complex on the exterior of the liposome may interact directly with the bulk water. Complexes loaded into the interior show quenched proton relaxation effects by slowed water exchange across the bilayer. Iron-based liposomes show increased T_2 relaxivity at high field strengths (>7 T), analogous to lanthanide-based liposomes. Studies of lanthanide(III)-loaded liposomes showed

additional susceptibility contributions to T_2 that increase with magnetic field strength, making them candidates for T_2 -based imaging procedures.⁵⁷

III. Design of redox-responsive transition metal MRI probes

Transition metal MRI probes must be highly kinetically resistant to metal ion release under physiological conditions. Thermodynamic stability is also important. Complexes that have large formation constants and are thus thermodynamically stable are desirable; however, kinetic inertness is also quite important as the resistance to dissociation can prevent equilibration with ligands found in the blood, such as transferrin for Fe(III).²⁷ Transition metal complexes of macrocycles,⁴⁴ self-assembled cages,⁶² or other types of rigid ligands^{63, 64} may offer a high degree of kinetic inertness towards release of the metal ion which is advantageous in probe development.

Other general considerations include the concentrations of MRI probes that are required for detection. Relaxivity (T_1) MRI probes are typically used in high micromolar concentrations.⁶ For example, if the tissue background proton relaxation time is 1 second, reduction of the signal by 10% would require 50 μ M contrast agent with a relaxivity 2.0 mM⁻¹s⁻¹. Relaxivity values for mononuclear Fe(III) probes are often close to 2.0 mM⁻¹s⁻¹ and are higher for multinuclear probes at 5.3 mM⁻¹s⁻¹ and 8.7 mM⁻¹s⁻¹ for dinuclear and tetranuclear Fe(III) complexes, respectively at 4.7 T and 37 °C in buffered solution.¹¹ By contrast, paraCEST agents require higher concentrations and are detectable in low millimolar concentrations in solution.⁶⁵ LipoCEST agents produce signal in nanomolar vesicle concentrations, but are loaded with high millimolar concentrations of complex.⁵³ The paraSHIFT agents are typically used in millimolar concentrations, although an optimized study with a lanthanide-based proton paraSHIFT probe reported imaging with probe injected by tail vein at 0.1 mmol/kg.⁶⁶ This dose is similar to that given for T_1 agents. Injections into animals with MRI contrast agents typically require good aqueous solubility to prepare stock solutions of 10-100 mM.⁶⁷

The electrode potential of the metal ion center can be modulated over a nearly 2 V range through modification of the ligand donor groups and resulting coordination environment. For example, as shown in Figures 5 and 6, macrocyclic complexes of Co and Fe have electrode potentials for the II/III couple that are tuned over a range of 1.2 to 2.1 volts, respectively. (All potentials are given versus NHE unless otherwise specified). Macrocyclic complexes of TACN (1,4,7-triazacyclonone) are featured here, although many other macrocyclic ligands have been reported for transition metal probes. 14 In general, complexes that remain in the divalent state in the biological environment are characterized by positive redox potentials (> 500 mV versus NHE) and complexes that remain in the trivalent state in a biological environment have negative redox potentials. The redox potentials of common biological oxidants and reductants that affect metal ion oxidation states are elaborated on further below. Ligands based on TACN with its small cavity size and favored six-coordination stabilize the trivalent state of iron¹¹ for pendants such as hydroxypropyl, 68 phosphonate 67 or phenolate. 69 For cobalt-based TACN complexes, pyrazole, 70 carboxylate pendants 41, 71 or ternary complexes containing acetylacetonate⁷² tend to stabilize the trivalent state. Amide pendant groups stabilize Co(II)⁴⁸ or Fe(II)⁷³ in TACN complexes or in dinuclear complexes with linear chelates.^{63, 64} Larger

macrocyclic backbones such as CYCLEN (1,4,7,10-tetraazacyclododecane) form eight- or seven-coordinate complexes and stabilize the divalent state in both cobalt and iron. CYCLAM (1,4,8,11-tetraazacyclotetradecane) ligands with four pendants typically form six-coordinate complexes with Co(II)/Co(III) or Fe(II) with intermediate redox potentials, $^{47, 74}$ as shown in Figures 5 and 6. Complexes that have mid-range redox potentials are complexes that are not strongly stabilized as either M(II) or M(III) may be useful in applications for redox sensing such as $[Co(CMP)]^{3+41}$ or $[Fe(PyC3A)].^{27}$

Finally, what is the desired redox potential of the MRI probe and what type of reactions are important for molecular imaging of redox imbalance? Redox imbalance characterizes many inflammatory diseases such as cancer, cardiovascular and bowel diseases, diabetes and arthritis. 19, 75 Inflammation typically involves oxidative stress which is defined as an imbalance between the production of oxidants and antioxidant defenses that may lead to damage in tissue. There are different approaches to develop probes for oxidative stress. Small molecules may buffer the redox status of tissue, especially in the intracellular environment, and such levels may vary for normal tissue compared to diseased states.^{22, 76} The probe might be designed to sense this redox state by reaction with one component of the buffer, for example glutathione (GSH) or its oxidized form, glutathione disulfide (GSSG). The concentration and ratio of the redox buffer pairs are, however, controlled enzymatically in a complex and wellintegrated system that is not always fully equilibrated.⁷⁷ A second approach is to consider the production of reactive oxygen (ROS) and reactive nitrogen species (RNS) that are present in elevated levels under inflammatory conditions. In this approach, probes are designed to undergo redox changes upon interaction with these reactive species based on considerations of the potentials of appropriate one electron redox reactions.⁷⁸ Redox biology is an extensively researched topic, and the reader is directed to recent reviews of these approaches. 17, 19, 75, 77, 79

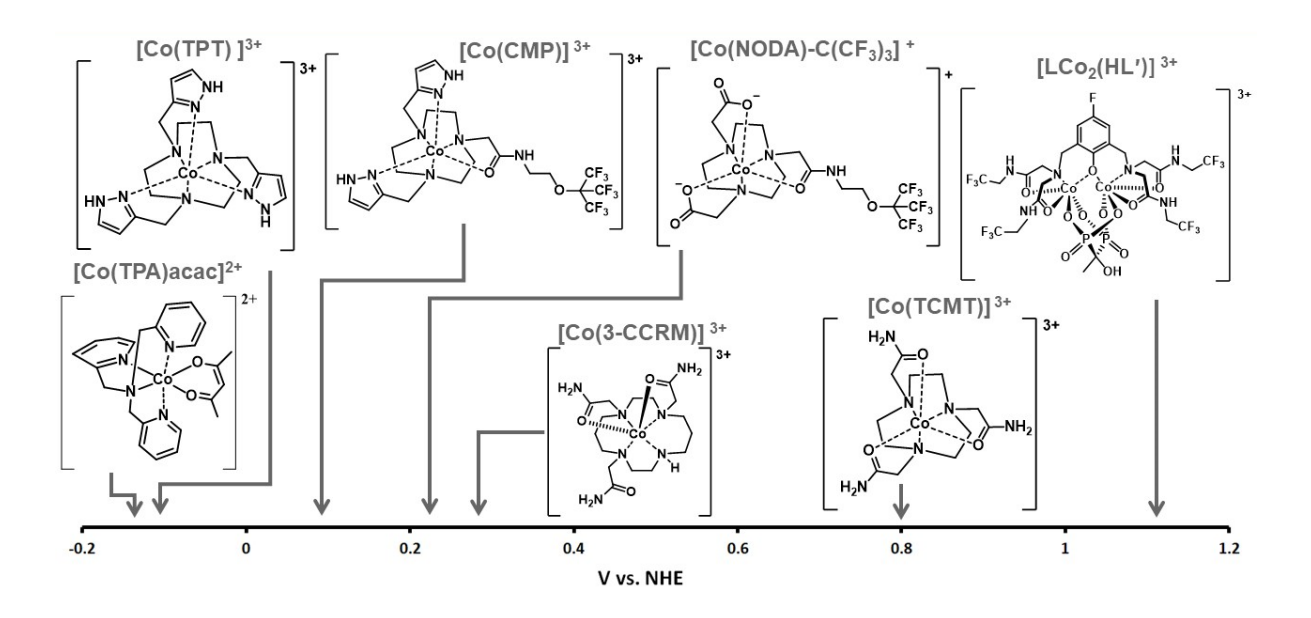


Figure 5. Electrode potentials for cobalt (Co³⁺/Co²⁺) complexes taken in aqueous solution at near neutral pH values. Charges are shown for the trivalent cobalt complexes.

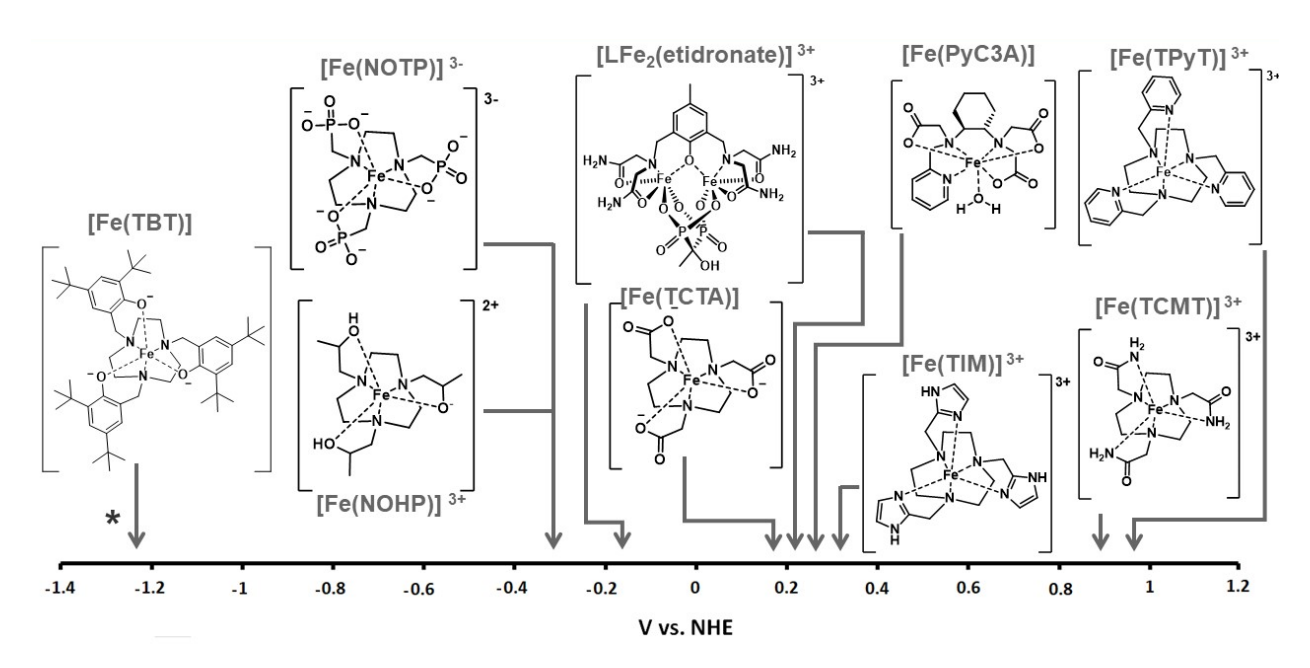


Figure 6. Electrode potentials for iron (Fe^{3+}/Fe^{2+}) complexes taken in aqueous solution at near neutral pH values. *The electrode potential of Fe(TBT) was reported in CH₃CN. Charges are shown for trivalent iron complexes.

It is important to note that the majority of contrast agents are extracellular fluid agents that extravasate from the vasculature into extracellular space and do not experience the intracellular environment.¹ This is important because the extracellular redox environment is

not as tightly controlled nor as well-defined as the intracellular environment.⁷⁷ For example, whereas the intracellular environment is set by several important redox couples including NAD⁺/NADH, the extracellular space lacks these thermodynamically equilibrated couples. Moreover, the intracellular environment is more reducing than the extracellular environment. Within the cytosol, the redox poise arises from the NAD+/NADH couple set at -240 mV, whereas the NADP+/NADPH system is set at -393 mV. In this case, both systems are thought to operate near equilibrium through enzyme-catalyzed reactions.⁷⁷ By contrast, the thiol/disulfide redox system operates at low flux and is not at equilibrium, but is more accurately considered to be part of a system of kinetically controlled sulfur switches. Such thiol switches include couples such as glutathione (GSH/GSSG), cysteine/cystine and proteins with multiple thiol groups as part of the redox-dependent thiol proteome.⁷⁹ A discussion of reaction kinetic restraints in redox reactions versus thermodynamically dictated redox regulation makes this point.⁸⁰ In other words, a description of redox biology as a system whereby molecules serve as redox buffers and that the concentrations and electrode potential of the couple contribute to the overall redox potential according to the Nernst equation is not a complete picture, as in some cases kinetics may be the limiting factor.77,80

Molecules that act as signaling agents such as superoxide (O_2^-) and peroxide (H_2O_2) enable the integration of redox systems and may serve as targets for detection, which we will consider here. 77, 81-83 These small molecule messengers along with their target membrane proteins coordinate intracellular with extracellular events and thus influence the extracellular environment.84 H₂O₂ is formed in mitochondrial respiration and by NADPH oxidase (NOX) enzymes that are found in the plasma membrane of phagocytes and endothelial cells that become upregulated during inflammatory processes.¹⁷ NADP oxidases activate O₂ for generation of superoxide (or in some cases, hydrogen peroxide) for phagocytic killing of pathogens in the extracellular space during inflammation.⁵⁴ Superoxide reacts to form hydrogen peroxide and oxygen through spontaneous dismutation or by SOD enzymes.¹⁷ During inflammation, macrophages and other phagocytotic cells that are part of the immune system response are recruited to create oxidative stress through a rise in superoxide and hydrogen peroxide levels as reactive oxygen species (ROS).¹⁷ Superoxide can also react with NO radical to produce peroxynitrite, (ONOO-), an example of a reactive nitrogen species. Extracellular enzymes that play key roles in inflammation include myeloperoxidases, as enzymes that are released by macrophages and neutrophils of the immune system, and glutathione peroxidase as protective enzymes which reduces peroxide to water and lipid hydroperoxide to alcohols.⁷⁹

Hydrogen peroxide is one of the primary molecules of interest for detection with chemical probes given its role as a signaling molecule that increases during inflammatory processes. While it is difficult to accurately measure concentrations of H_2O_2 in humans, concentrations of peroxide in the blood are likely in the range of 1-5 μ M and may increase to 30-50 μ M during chronic inflammation. These levels may potentially be assessed by using relaxivity-based MRI probes that produce signal at micromolar concentrations. Transition metal complexes (Fe(II), Co(II), Ni(II), Cu(II)) with redox potentials between 100 to 300 mV versus NHE

are oxidized by hydrogen peroxide and in the presence of ascorbate as reductant produce ROS as monitored by biomolecule cleavage. ⁸⁶ One electron potentials are used here to describe hydrogen peroxide acting as an oxidant of the reduced divalent state of the metal complex $(H_2O_2, H^+/HO^\bullet, OH_2 E_0 = 0.39 \text{ V}, \text{pH 7}, 298 \text{ K versus NHE})$. Given that hydrogen peroxide is a relatively weak oxidant, some of the probes described below are only oxidized in the presence of peroxidases and H_2O_2 which produce more reactive ROS such as hypochlorous acid. ^{41,87} High levels of myeloperoxidases in sites of inflammation support this approach. ⁸⁸

Another molecule of interest which is critical to metabolic processes within cells and as a precursor to superoxide is molecular O_2 . Oxygen is dissolved in the blood in low millimolar amounts with arterial blood levels of 0.17 mM O_2 and lower levels in hypoxic regions of 17 μ M.⁸⁹ Hypoxia is prevalent in tumors as the vasculature tends to be chaotic and underdeveloped due to the rapid growth of the tumor.⁹⁰ Hypoxia is connected to increased oxidative stress and proliferation through effects on the upregulation of the transcription factor hypoxia-inducible factors (HIF).⁸³ For this reason, there is renewed interest in the design of probes for O_2 levels including for MRI as well as other imaging modalities.⁹¹ Given the O_2/O_2 -potential of -0.19 V, complexes that are oxidized by molecular oxygen typically have M^{n+1}/M^{n+1} redox potentials that are negative, in the range of -0.19 V or less. For example, a Co(II) complex⁷⁰ and a dinuclear Fe(II) complex⁶³ with negative redox potentials are both oxidized by O_2 to provide a redox responsive agent as discussed below.

Other ROS species are poorer targets for probes. The hydroxy radical which may be produced by reaction of peroxide with reducing metal ions in the Fenton reaction is a much stronger oxidant than peroxide, but is very reactive and has a short lifetime in solution. Similarly, the superoxide radical requires two protons and an electron to be an oxidant and this kinetically slow reaction contributes to the importance of the enzymatic dismutation of superoxide. Instead, the superoxide radical may behave as a weak reductant. Other reductants that are important in extracellular space include ascorbate with an electrode potential of 0.28 mV versus NHE.

IV. Transition metal complexes for redox-responsive probe development

Coordination complexes of Co(II)/Co(III). The Co(II)/(III) redox couple is tunable over greater than 1.2 V (Figure 5). Bioinorganic researchers have long utilized this couple to capitalize on the marked difference in lability of the two oxidation states. For example, Co(III) complexes have a large degree of kinetic inertness and are used for the delivery of drugs or to function as warheads, and are complemented by the lability of Co(II) complexes formed under reducing conditions inside of the cell. For MRI probes, the shift properties of the Co(II) center are useful to prepare paraCEST, paraSHIFT, or lipoCEST agents. High-spin Co(II) complexes produce large hyperfine shifts and give highly dispersed proton resonances with relatively narrow line widths (Figure 2).

Our initial foray into Co(II) paraCEST agents featured complexes with amide pendants, such as [Co(TCMT)]²⁺ and other analogs that were stabilized in the divalent form for paraCEST applications (Figure 5).⁴⁸ Co(II) complexes with the CYCLAM ligand and four amide pendant groups were studied as pH-sensitive probes by following the intensity of multiple CEST peaks due to amide NH proton exchange. 45 Similarly, dinuclear Co(II) complexes (LCo₂(HL')) are stabilized in the divalent form and have applications as pH- based ratiometric probes.⁶⁴ To lower the redox potential to create responsive agents based on macrocyclic complexes, pyrazole pendants were used to produce the [Co(TPT)]²⁺ complex.⁷⁰ The Co(II) form of this complex produced a sharp CEST peak at 135 ppm versus bulk water. This complex had a negative electrode potential ($E_0 = -107 \text{ mV}$) and reacted readily with O_2 to give the diamagnetic Co(III) complex which could be reduced back to Co(II) with dithionite or cysteine. A secondorder rate constant for oxidation of the complex was determined and used to calculate the halflife of the complex at different O₂ pressures in the absence of other oxidants. These calculations showed that the reduced [Co(TPT)]²⁺ complex had a half-life of 2.6 hours in arterial blood, but a half-life of 26 hours in hypoxic tumors. Shorter half-lives upon reaction with O2 are desirable for in vivo measurements of hypoxia. Another drawback of this probe is that other oxidants such as hydrogen peroxide also catalyze oxidation, so that the probe is not specific for O₂ registration.

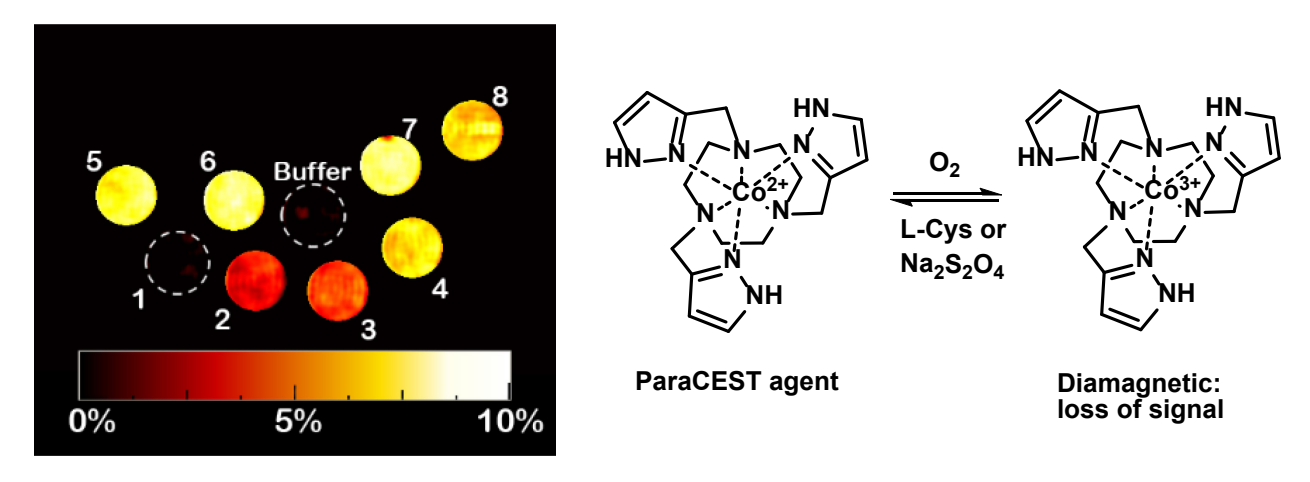


Figure 7. A paraCEST switch based on Co(II)/Co(III). MRI phantoms from CEST at -135 ppm, 37 ° C at 4.7 T: [Co(TPT)]³⁺ and the following equiv of dithionite: none (1), 0.25 equiv (2), 0.38 equiv. (3); 0.50 equiv. (4); 0.75 equiv. (5); 1.0 equiv. (6) 1.25 equiv. (7); [Co(TPT)]²⁺ (8). Adapted from ref. 69 with permission. Copyright 2013 Wiley

Co(II) complexes of derivatives of TACN with positive electrode potentials (150-200 mV) were reported by the Que group for 19 F paraSHIFT studies. 94 These complexes had fluorine tails in close proximity to the Co(II) center for producing a shift in the 19 F resonance and an increase in 19 F relaxation rates. While both complexes reacted with H_2O_2 , the complex with two pyrazole pendants [(Co(CMP))] $^{2+}$ reacted more readily with peroxide, whereas the probe with two carboxylate groups ([Co(CMA)]) oxidizes only when treated with peroxide and

peroxidases.⁴¹ A second way to create Co(II) complexes with electrode potentials in the 200-400 mV range is to use the cyclam backbone. For example, [Co(3-CCRM)]²⁺ has a redox potential of 290 mV versus NHE (Figure 5).⁷⁴

Co(II) complexes show only a small effect on water proton relaxation ($r_1 < 0.1 \text{ mM}^{-1}\text{s}^{-1}$),⁷² yet a switch between Co(III)/Co(II) in a derivative of the [Co(TPA)(acac)]²⁺ complex was successfully used to probe tumor spheroid hypoxia by monitoring changes in relaxivity.⁹⁵ A series of Co(III) complexes were taken up in the tumor cells upon reduction to the Co(II) form of the complex under hypoxic conditions. Differences in uptake into necrotic regions were observed and the proton relaxation times were modulated in the heterogeneous environment of the tumor.

Co(II) complexes of CYCLAM with hydroxypropyl pendants produce lipoCEST agents. 54 Liposomes containing complexes loaded into the interior of the liposome and in the bilayer produced a lipoCEST peak at physiologically relevant osmolality (300 mOs/L). The position of the CEST peak is dependent on the complex and its concentration inside of the liposome and the presence of amphiphilic Co(II) complexes in the bilayer. The tunability of the redox potential of the Co(II)/(III) center and our report on Co(II)-based lipoCEST agents suggests that redox-responsive liposomes are ripe for development. Recently, liposome-based photoacoustic probes have been reported that are responsive to H_2O_2 produced in inflammatory processes including tumors and sites of bacterial infection. 96

Coordination complexes of Fe(II)/Fe(III). Iron has much promise as a redox-responsive MRI probe given that both Fe(II) and Fe(III) have paramagnetic spin states. High spin Fe(II) is a paraCEST agent in macrocyclic complexes with pendants such as amide or amino-pyridine groups (Figure 6). 36, 47, 97 These complexes are stabilized as Fe(II). Interestingly, Fe(II) paraCEST and paraSHIFT agents that capitalize on spin-state crossover as a function of temperature have been reported. 37, 42 As the Fe(II) complexes go from low to high spin, the paraCEST peaks shift and increase in intensity to give some of the best temperature dependent probes reported to date. Similarly, the ¹⁹F resonance changes with temperature for the paraSHIFT agent as the high spin state of Fe(II) is populated. Aside from the temperature dependent spin-crossover, the paraCEST properties of Fe(II) are often similar to those observed for the Co(II) analogs. 14

Low-spin Fe(III) paraCEST agents are of interest as they may lead to a paraCEST redox-responsive ratiometric couple (high spin Fe(II)/low spin Fe(III)). One such low- spin Fe(III) complex had three imidazole pendants, Fe(TIM), and a redox potential of 315 mV at pH $6.5.^{98,\,99}$ As the imidazole pendants deprotonate, the electrode potential of the complex becomes more negative (-270 mV at pH 12), signifying stabilization of Fe(III) with increasing the number of anionic pendant groups. This complex, as a low-spin Fe(III) probe has sharp proton resonances which are not as highly dispersed as those of high spin Fe(II) as expected from the lower magnetic susceptibility of Fe(III). Thus, the CEST peak of the imidazole of the Fe(III) complex of TIM is not very highly shifted from the water peak (8 ppm). The Fe(II) form of the TIM complex oxidizes slowly with O_2 in the air, O_2 suggesting further applications as an oxygen or

peroxide responsive probe. Other pendants such as phosphinates or hydroxyalkyl groups on the TACN macrocycle form complexes of [Fe(NOPH)]²⁺ or [Fe(NOTP)]³⁻ that are stabilized in the trivalent, high-spin state and are not candidates for development as redox-responsive MRI probes.^{67, 100}

Dinuclear Fe complexes have been studied as redox probes in a system that produces an unusual ratiometric couple. 63 The Fe₂(L)(etidronate) series has Fe(II)/Fe(II), Fe(II)/Fe(III), and Fe(III)/Fe(III) oxidation states. In this case, both Fe(II) centers are high spin and the Fe(II)/Fe(III) complex features magnetically coupled iron centers that result in shortened electronic relaxation times to produce a paraCEST agent. These are rare examples of ratiometric MRI probes that produce distinct CEST peaks for both oxidation states. Electrochemical methods were used to produce the various oxidation state combinations, but the Fe(II)/Fe(II) complex could also be converted to the Fe(II)/Fe(III) complex by air oxidation.

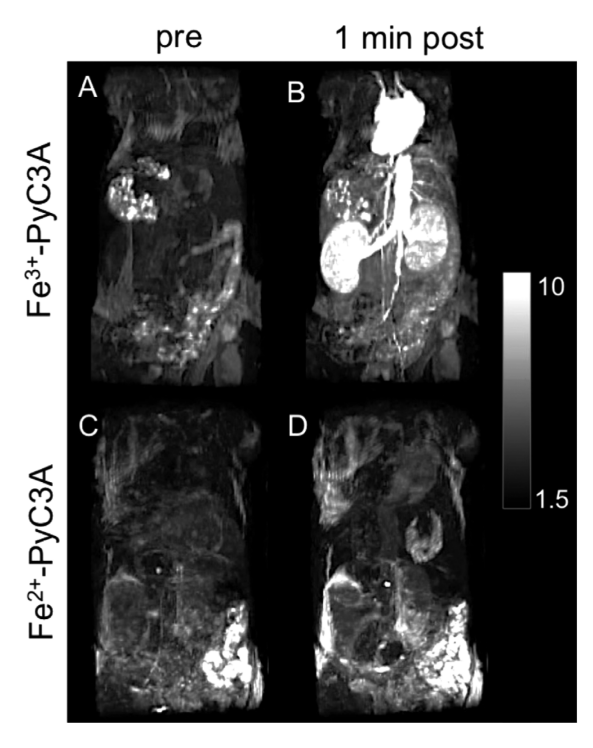


Figure 8. Fe(II)/Fe(III) MRI probes employed for detecting pancreatitis by T_1 weighted imaging. Reprinted from ref. 26 with permission. Copyright 2019 American Chemical Society.

A remarkable study lead by Gale featured conversion of high-spin Fe(II) to high-spin Fe(III) upon oxidation of [(Fe(PyC3A)] with hydrogen peroxide.²⁷ This complex has an electrode potential of 230 mV versus NHE and the Fe(II) form was rapidly oxidized by H₂O₂. Both Fe(II) and Fe(III) complexes shorten proton relaxation times, but the Fe(III) center was approximately 10-fold more active as a T_1 agent. This article demonstrated one of the few in vivo applications with a transition metal coordination complex as a redox-responsive probe. The iron complexes were used to image inflammation in the pancreas (pancreatitis), which was induced artificially by addition of lipopolysaccharide (LPS). Gale's group has used analogous Fe(III) complexes with mixed acetate and nitrogen heterocycle pendants to switch between mononuclear Fe(III) complexes with an inner-sphere water and µhydroxy-bridged dinuclear Fe(III) complexes of lowered relaxivity through either enzymatic 101 or pH- driven²⁸ reactions.

Iron macrocyclic complexes have been incorporated into liposomes to produce nanoparticle-based CEST, T_1 and T_2 agents. The iron complexes in the interior and bilayer of these liposomes were high-spin Fe(III) complexes. The r_1 relaxivity of the iron loaded liposomes was used to track the probes in T_1 -weighted mice MRI studies. The CEST effect was modest even in shrunken liposomes which was expected because high-spin Fe(III) complexes, unlike Co(II) complexes, are not shift agents. While liposomal

systems with Fe(II)/Fe(III) switches are not yet reported, one could imagine using the change in T_1 or T_2 proton relaxation times to track oxidation state changes. Liposomes may be useful in other ways to transport responsive agents. For example, studies with Eu(II)/Eu(III) liposomal systems highlight the promise of protecting the easily oxidized divalent complexes from the environment by using liposomal nanoparticles as carriers.¹⁰²

Additional first-row transition metal probes. Other first-row transition metal ion complexes from Table 1 that have been used as redox-responsive MRI probes include Mn(II)/Mn(III) and Cu(II)/Cu(I) and will be discussed briefly here. Notably, Ni(II) has been used for its paramagnetic shift properties both as a paraCEST agent and a paraSHIFT agent, 40, 47, 103 but is only present in the divalent state under physiological conditions. However, it is worth noting that spin-state changes produced upon going from low-spin square planar to high-spin octahedral geometry can be triggered by association/dissociation of ligands through light or pH-induced changes. 104

Some of the earliest reported MRI redox-responsive probes contained the Mn(II)/Mn(III) couple in complexes with porphyrin ligands. Since then, several other probes have been reported including an interesting example of a Janus switched probe wherein the ligand donor groups change with oxidation state change. These probes showed a decrease in proton relaxivity by a factor of about three-fold upon oxidation to the Mn(III) state. Mn(II) probes that react with hydrogen peroxide at a ligand group or at the metal center have been recently reviewed. Mn(II)/(III) complexes have also been studied as NO responsive probes through changes in relaxivity in the two oxidation states. Mn

Redox activated Cu(II)/Cu(I) agents have been reported for MRI probe development. One study measured water proton relaxation in solution and showed that oxidation of a Cu(I) complex gave a Cu(II) complex with modest relaxivity values.¹⁰⁹ A second set of studies followed the change in the ¹⁹F NMR signal of fluorinated Cu(II) probes to show that the reduced Cu(I) species is produced under hypoxic conditions in cell culture studies.¹¹⁰ A third study demonstrated that a dinuclear Cu(II) complex with magnetic exchanging coupling between the two copper centers has relatively sharp proton resonances and a CEST peak from NH proton exchange.¹¹¹

V. Outlook for in vivo studies

First-row transition metal complexes show promise as redox-responsive MRI probes. Their electrode potentials are modulated by choice of donor ligands and coordination geometry and are easily varied over a large range. In solution, oxidation state changes of the MRI probe are readily detected through changes in probe signal, but there are additional considerations for more challenging in vivo applications. To optimize the response, a large difference in signal for the two states of the responsive probe is desirable.^{6, 8} Some of the probes described here have more favorable properties than others. For relaxivity probes, conversion of Mn(II) to Mn(III) complexes results in reduced relaxivity upon oxidation with hydrogen peroxide, with

relaxivity changes of typically about three-fold. Moreover, a decrease in signal upon treatment with the oxidant of interest is not desirable for a responsive probe. In contrast, the high-spin Fe(II) to high-spin Fe(III) switch produced a ten-fold difference in signal with increased relaxivity upon oxidation. This probe was successfully used for in vivo imaging of inflammation in mice. For relaxivity probes based on Co(II) or Cu(II), compared to the diamagnetic analogs (Co(III) or Cu(I)), the signal change is not large based on the already poor water proton T_1 shortening of these divalent ions compared to background. A general disadvantage of the redox-responsive relaxivity probes that rely on T_1 changes is that it is difficult to prepare a ratiometric probe. Ratiometric probes enable the separation of the concentration effects from the responsive nature of the probe. One promising approach involves monitoring the ratio of T_1 to T_2 relaxation times as a means of distinguishing probe concentration and response.

For responsive probes that contain paramagnetic shift agents, it is more straightforward to produce ratiometric probes if the two oxidation states of the probe produce distinct signals so that both species can be tracked. For example, the high-spin Fe(II)/ low-spin Fe(III) couple presents an opportunity for a ratiometric paraCEST agent, as both are shift agents. ^{63, 98} However, paraCEST probes of Co(II) suffer from the Co(III) state being diamagnetic and silent so that it cannot be monitored by MRI as a paraCEST probe, although technically it may be a diamagnetic CEST probe. ⁷⁰ Alternatively, paraSHIFT agents based on ¹H or ¹⁹F NMR resonances may potentially be ratiometric if both oxidation states of the metal ion complex produce distinct resonances. ^{33, 113} LipoCEST probes may also be ratiometric because the position and intensity of the CEST peak will depend on the concentration and nature of paramagnetic species in the interior and in the bilayer. ⁵¹ Notably, relaxivity agents tend to destroy the CEST or paraSHIFT signal through broadening of nuclear resonances, making it challenging to include both contrast mechanisms in a probe. A responsive probe that shows a switched on CEST effect upon changing the T₁ relaxation of bulk water protons has been reported. ¹¹⁴

To date, there are few studies that use redox-responsive transition metal coordination complexes as MRI probes in vivo. We attribute this fact to several key challenges to address including probe sensitivity that needs to correspond to the low concentration of oxidant, the need to target the probes to the site of interest and to control pharmacokinetic distribution and clearance. For example, the high concentrations required for paraCEST agents limits their use in vivo, whereas nanoparticle CEST agents and relaxivity agents require lower concentrations. ⁴⁹ Hydrogen peroxide is available in the extracellular matrix in micromolar concentrations and so a probe needs to produce signal in this concentration range to monitor physiological or pathological conditions though MRI methods. Also, animal models for diseases that involve inflammatory processes should be pursued in future applications, in preference to artificially induced inflammation such as injection of LPS into mice.²⁷ Various photoacoustic, fluorescent, or radioisotope probes have been shown to register ROS derived inflammation in mouse models including tumors, ¹⁹ bacterial infections, ⁹⁶ or atherosclerosis. ^{19, 115} A recently reported

Gd(III)-based MRI probe for myeloperoxidase activity showed improved contrast of unstable atherosclerotic plaque in mice. 116

Once the animal model is chosen, the reactive probe must distribute to the site of inflammation. Small molecule hydrophilic coordination complexes generally behave as extracellular fluid agents and clear the body rapidly. The kinetics of distribution and clearance needs to be balanced with the kinetics for oxidation or reduction. Most small molecules clear mice within 30 minutes and are not retained in tumors or other sites of inflammation for extended times. For greater retention in tumors, the enhanced permeability and retention effect for extravasation of 50-100 nm-sized nanoparticles into tumors suggests that MRI probes based on liposomes would be effective. 117 For example, Gd(III)-based liposomal contrast agents have been shown to be taken up and retained in tumor tissue.⁵⁹ For stroke or atherosclerosis, cancer or liver injury, attachment of the MRI probe to a peptide that recognizes fibrin has used for Gd(III)-based probes. 6 Other targeting strategies such as using contrast agents with hydrazine groups that can cross-link to aldehydes on inflammation damaged extracellular matrix proteins might be pursued. 118 Thus, modifications of the transition metal complex to distribute the probe to the site of interest may be important. These targeting approaches have been used successfully with Gd(III) agents that are always on⁶; first-row transition metal agents that are responsive by producing a modified signal in a site of inflammation may be especially powerful as responsive probes.

Acknowledgements. JRM thanks the NSF (CHE-2004135) for support of our research on cobalt and iron redox-activated MRI probes.

Notes. JRM is cofounder of Ferric Contrast, a company that develops iron-based MRI contrast agents.

References

- (1) Wahsner, J.; Gale, E. M.; Rodriguez-Rodriguez, A.; Caravan, P. Chemistry of MRI Contrast Agents: Current Challenges and New Frontiers. *Chem Rev* **2019**, *119* (2), 957-1057.
- (2) Boros, E.; Gale, E. M.; Caravan, P. MR imaging probes: design and applications. *Dalton Trans* **2015**, *44* (11), 4804-4818.
- (3) Pierre, V. r. C.; Allen, M. J. *Contrast agents for MRI : experimental methods*; Royal Society of Chemistry, 2018.
- (4) Merbach, A.; Helm, L.; Toth, E. *The Chemistry of Contrast Agents in Medical Magnetic Resonance Imaging, second ed.*; Wiley & sons, 2013.
- (5) Li, H.; Meade, T. J. Molecular magnetic resonance imaging with Gd (III)-based contrast agents: challenges and key advances. *J Am Chem Soc* **2019**, *141* (43), 17025-17041.
- (6) Shuvaev, S.; Akam, E.; Caravan, P. Molecular MR Contrast Agents. Invest Radiol 2021, 56 (1), 20-34.
- (7) Lacerda, S. Targeted Contrast Agents for Molecular MRI. *Inorganics* **2018**, 6 (4).

- (8) Bonnet, C. S.; Toth, E. Metal-based environment-sensitive MRI contrast agents. *Curr Opin Chem Biol* **2021**, *61*, 154-169.
- (9) a) De Leon-Rodriguez, L. M.; Lubag, A. J.; Malloy, C. R.; Martinez, G. V.; Gillies, R. J.; Sherry, A. D. Responsive MRI agents for sensing metabolism in vivo. *Acc Chem Res* **2009**, *42* (7), 948-957. b) Yoo, B.; Pagel, M. D. An overview of responsive MRI contrast agents for molecular imaging. *Front Biosci* **2008**, *13*, 1733-1752.
- (10) Gupta, A.; Caravan, P.; Price, W. S.; Platas-Iglesias, C.; Gale, E. M. Applications for transition-metal chemistry in contrast-enhanced magnetic resonance imaging. *Inorg Chem* **2020**, *59* (10), 6648-6678.
- (11) Kras, E. A.; Snyder, E. M.; Sokolow, G. E.; Morrow, J. R. The Distinct Coordination Chemistry of Fe(III)-based MRI Probes. *Acc. Chem. Res.* **2022**, *55*, 1435-1444.
- (12) Baranyai, Z.; Carniato, F.; Nucera, A.; Horvath, D.; Tei, L.; Platas-Iglesias, C.; Botta, M. Defining the conditions for the development of the emerging class of Fe(III)-based MRI contrast agents *Chem. Sci.* **2021**, *12*, *11138-11145*.
- (13) Botta, M.; Carniato, F.; Esteban-Gómez, D.; Platas-Iglesias, C.; Tei, L. Mn (II) compounds as an alternative to Gd-based MRI probes. *Future Med Chem* **2019**, *11* (12), 1461-1483.
- (14) Morrow, J. R. C., M. S. I.; Abozeid, S. M.; Patel, A.; Raymond, J. J. Transition metal ParaCEST, LipoCEST and CellCEST agents as MRI probes. In *Encyclopedia of Inorganic and Bioinorganic Chemistry*; Storr, R. A. S. a. T., Ed.; John Wiley & Sons, 2020; pp 1-19.
- (15) Karbalaei, S.; Goldsmith, C. R. Recent advances in the preclinical development of responsive MRI contrast agents capable of detecting hydrogen peroxide. *J Inorg Biochem* **2022**, *230*, 111763.
- (16) a) Do, Q. N.; Ratnakar, J. S.; Kovacs, Z.; Sherry, A. D. Redox- and Hypoxia-Responsive MRI Contrast Agents. *Chemmedchem* **2014**, *9* (6), 1116-1129. b) Tsitovich, P. B.; Burns, P. J.; Mckay, A. M.; Morrow, J. R. Redox-activated MRI contrast agents based on lanthanide and transition metal ions. *J Inorg Biochem* **2014**, *133*, 143-154.
- (17) Mittal, M.; Siddiqui, M. R.; Tran, K.; Reddy, S. P.; Malik, A. B. Reactive Oxygen Species in Inflammation and Tissue Injury. *Antioxid Redox Sign* **2014**, *20* (7), 1126-1167.
- (18) a) Sosa, V.; Moline, T.; Somoza, R.; Paciucci, R.; Kondoh, H.; LLeonart, M. E. Oxidative stress and cancer: An overview. *Ageing Res Rev* **2013**, *12* (1), 376-390. b) Chen, L.; Deng, H.; Cui, H.; Fang, J.; Zuo, Z.; Deng, J.; Li, Y.; Wang, X.; Zhao, L. Inlfammatory responses and inflammation-associated diseases in organs. *Oncotarget* **2018**, *9* (6), 7204-7218.
- (19) Jones, M. A.; MacCuaig, W. M.; Frickenstein, A. N.; Camalan, S.; Gurcan, M. N.; Holter-Chakrabarty, J.; Morris, K. T.; McNally, M. W.; Booth, K. K.; Carter, S.; et al. Molecular Imaging of Inflammatory Disease. *Biomedicines* **2021**, *9*, 152.
- (20) Bertini, I.; Turano, P.; Vila, A. J. Nuclear-Magnetic-Resonance of Paramagnetic Metalloproteins. *Chem Rev* **1993**, *93* (8), 2833-2932.
- (21) Viswanathan, S.; Kovacs, Z.; Green, K. N.; Ratnakar, S. J.; Sherry, A. D. Alternatives to Gadolinium-Based Metal Chelates for Magnetic Resonance Imaging. *Chem Rev* **2010**, *110* (5), 2960-3018.
- (22) Pinto, S. M.; Tome, V.; Calvete, M. J. F.; Castro, M. M. C. A.; Toth, E.; Geraldes, C. F. G. C. Metalbased redox-responsive MRI contrast agents. *Coordin Chem Rev* **2019**, *390*, 1-31.
- (23) Lancelot, E.; Raynaud, J.-S.; Desché, P. Current and future MR contrast agents: seeking a better chemical stability and relaxivity for optimal safety and efficacy. *Invest Radiol* **2020**, *55* (9), 578-588.
- (24) Bertini, I.; Luchinat, C.; Parigi, G.; Ravera, E. NMR of Paramagnetic Molecules Applications to Metallobiomolecules and Models SECOND EDITION INTRODUCTION. *NMR of Paramagnetic Molecules:* Applications to Metallobiomolecules and Models, 2nd Edition **2017**, 1-24.
- (25) Caravan, P.; Esteban-Gómez, D.; Rodríguez-Rodríguez, A.; Platas-Iglesias, C. Water exchange in lanthanide complexes for MRI applications. Lessons learned over the last 25 years. *Dalton Trans* **2019**, *48* (30), 11161-11180.

- (26) Caravan, P.; Ellison, J. J.; McMurry, T. J.; Lauffer, R. B. Gadolinium (III) chelates as MRI contrast agents: structure, dynamics, and applications. *Chem Rev* **1999**, *99* (9), 2293-2352.
- (27) Wang, H.; Jordan, V. C.; Ramsay, I. A.; Sojoodi, M.; Fuchs, B. C.; Tanabe, K. K.; Caravan, P.; Gale, E. M. Molecular magnetic resonance imaging using a redox-active iron complex. *J Am Chem Soc* **2019**, *141* (14), 5916-5925.
- (28) Wang, H.; Wong, A.; Lewis, L. C.; Nemeth, G. R.; Jordan, V. C.; Bacon, J. W.; Caravan, P.; Shafaat, H. S.; Gale, E. M. Rational Ligand Design Enables pH Control over Aqueous Iron Magnetostructural Dynamics and Relaxometric Properties. *Inorg Chem* **2020**, *59* (23), 17712-17721.
- (29) Schneppensieper, T.; Seibig, S.; Zahl, A.; Tregloan, P.; van Eldik, R. Influence of chelate effects on the water-exchange mechanism of polyaminecarboxylate complexes of iron (III). *Inorg Chem* **2001**, *40* (15), 3670-3676.
- (30) Caravan, P.; Farrar, C. T.; Frullano, L.; Uppal, R. Influence of molecular parameters and increasing magnetic field strength on relaxivity of gadolinium-and manganese-based T1 contrast agents. *Contrast Media Mol I* **2009**, *4* (2), 89-100.
- (31) Burns, P. J.; Cox, J. M.; Morrow, J. R. Imidazole-Appended Macrocyclic Complexes of Fe(II), Co(II), and Ni(II) as ParaCEST Agents. *Inorg Chem* **2017**, *56* (8), 4545-4554.
- (32) Martin, B.; Autschbach, J. Kohn-Sham calculations of NMR shifts for paramagnetic 3d metal complexes: protocols, delocalization error, and the curious amide proton shifts of a high-spin iron(II) macrocycle complex. *Phys Chem Chem Phys* **2016**, *18* (31), 21051-21068.
- (33) Blahut, J.; Benda, L.; Kotek, J.; Pintacuda, G.; Hermann, P. Paramagnetic Cobalt(II) Complexes with Cyclam Derivatives: Toward F-19 MRI Contrast Agents. *Inorg Chem* **2020**, *59* (14), 10071-10082.
- (34) Tsitovich, P. B.; Morrow, J. R. Macrocyclic ligands for Fe(II) paraCEST and chemical shift MRI contrast agents. *Inorg Chim Acta* **2012**, *393*, 3-11.
- (35) Tsitovich, P. B.; Cox, J. M.; Benedict, J. B.; Morrow, J. R. Six-coordinate Iron(II) and Cobalt(II) paraSHIFT Agents for Measuring Temperature by Magnetic Resonance Spectroscopy. *Inorg. Chem.* **2016**, *55*, 700-716.
- (36) Tsitovich, P. B.; Cox, J. M.; Spernyak, J. A.; Morrow, J. R. Gear Up for a pH Shift: A Responsive Iron(II) 2-Amino-6-picolylAppended Macrocyclic paraCEST Agent That Protonates at a Pendent Group. *Inorg Chem* **2016**, *55* (22), 12001-12010.
- (37) Jeon, I. R.; Park, J. G.; Haney, C. R.; Harris, T. D. Spin crossover iron(II) complexes as PARACEST MRI thermometers. *Chem Sci* **2014**, *5* (6), 2461-2465.
- (38) Harnden, A. C.; Parker, D.; Rogers, N. J. Employing paramagnetic shift for responsive MRI probes. *Coordin Chem Rev* **2019**, *383*, 30-42.
- (39) a) Srivastava, K.; Ferrauto, G.; Young, V. G.; Aime, S.; Pierre, V. C. Eight-Coordinate, Stable Fe(II) Complex as a Dual F-19 and CEST Contrast Agent for Ratiometric pH Imaging. *Inorg Chem* **2017**, *56* (20), 12206-12213. D b) Srivastava, K.; Weitz, E. A.; Peterson, K. L.; Marjanska, M.; Pierre, V. C. Fe- and Ln-DOTAm-F12 Are Effective Paramagnetic Fluorine Contrast Agents for MRI in Water and Blood. *Inorg Chem* **2017**, *56* (3), 1546-1557. b) Yu, M.; Bouley, B. S.; Xie, D.; Que, E. L. Highly fluorinated metal complexes as dual F-19 and PARACEST imaging agents. *Dalton Trans* **2019**, *48* (25), 9337-9341. c) Yu, M.; Xie, D.; Phan, K. P.; Enriquez, J. S.; Luci, J. J.; Que, E. L. A Co-II complex for F-19 MRI-based detection of reactive oxygen species. *Chem Commun* **2016**, *52* (96), 13885-13888.
- (40) Blahut, J.; Bernasek, K.; Galisova, A.; Herynek, V.; Cisarova, I.; Kotek, J.; Lang, J.; Matejkova, S.; Hermann, P. Paramagnetic F-19 Relaxation Enhancement in Nickel(II) Complexes of N-Trifluoroethyl Cyclam Derivatives and Cell Labeling for F-19 MRI. *Inorg Chem* **2017**, *56* (21), 13337-13348.
- (41) Yu, M.; Bouley, B. S.; Xie, D.; Enriquez, J. S.; Que, E. L. F-19 PARASHIFT Probes for Magnetic Resonance Detection of H2O2 and Peroxidase Activity. *J Am Chem Soc* **2018**, *140* (33), 10546-10552.

- (42) Thorarinsdottir, A. E.; Gaudette, A. I.; Harris, T. D. Spin-crossover and high-spin iron(II) complexes as chemical shift F-19 magnetic resonance thermometers. *Chem Sci* **2017**, *8* (3), 2448-2456.
- (43) Zhang, S. R.; Merritt, M.; Woessner, D. E.; Lenkinski, R. E.; Sherry, A. D. PARACEST agents: Modulating MRI contrast via water proton exchange. *Acc Chem Res* **2003**, *36* (10), 783-790.
- (44) Dorazio, S. J.; Olatunde, A. O.; Tsitovich, P. B.; Morrow, J. R. Comparison of divalent transition metal ion paraCEST MRI contrast agents. *J Biol Inorg Chem* **2014**, *19* (2), 191-205.
- (45) Bond, C. J.; Cineus, R.; Nazarenko, A. Y.; Spernyak, J. A.; Morrow, J. R. Isomeric Co(ii) paraCEST agents as pH responsive MRI probes. *Dalton T* **2020**, *49* (2), 279-284.
- (46) Abozeid, S. M.; Snyder, E. M.; Tittiris, T. Y.; Steuerwald, C. M.; Nazarenko, A. Y.; Morrow, J. R. Innersphere and outer-sphere water interactions in Co (II) paraCEST agents. *Inorg Chem* **2018**, *57* (4), 2085-2095.
- (47) Olatunde, A. O.; Bond, C. J.; Dorazio, S. J.; Cox, J. M.; Benedict, J. B.; Daddario, M. D.; Spernyak, J. A.; Morrow, J. R. Six, Seven or Eight Coordinate Fe-II, Co-II or Ni-II Complexes of Amide-Appended Tetraazamacrocycles for ParaCEST Thermometry. *Chem-Eur J* **2015**, *21* (50), 18290-18300.
- (48) Dorazio, S. J.; Olatunde, A. O.; Spernyak, J. A.; Morrow, J. R. CoCEST: cobalt(II) amide-appended paraCEST MRI contrast agents. *Chem Commun* **2013**, *49* (85), 10025-10027.
- (49) Sherry, A. D.; Castelli, D. D.; Aime, S. Prospects and limitations of paramagnetic chemical exchange saturation transfer agents serving as biological reporters in vivo. *Nmr Biomed* **2022**. DOI: ARTN e4698 10.1002/nbm.4698.
- (50) Carniato, F.; Ferrauto, G.; Munoz-Ubeda, M.; Tei, L. Water Diffusion Modulates the CEST Effect on Tb(III)-Mesoporous Silica Probes. *Magnetochemistry* **2020**, *6*, 38.
- 10.3390/magnetochemistry6030038. Ferrauto, G.; Carniato, F.; Tei, L.; Hu, H.; Aime, S.; Botta, M. MRI nanoprobes based on chemical exchange saturation transfer: Ln(III) chelates anchored on the surface of mesoporous silica nanoparticles. *Nanoscale* **2014**, *6* (16), 9604-9607.
- (51) Castelli, D. D.; Terreno, E.; Longo, D.; Aime, S. Nanoparticle-based chemical exchange saturation transfer (CEST) agents. *Nmr Biomed* **2013**, *26* (7), 839-849.
- (52) Bar-Shir, A.; Gilad, A. A.; Chan, K. W. Y.; Liu, G. S.; van Zijl, P. C. M.; Bulte, J. W. M.; McMahon, M. T. Metal Ion Sensing Using Ion Chemical Exchange Saturation Transfer F-19 Magnetic Resonance Imaging. *J Am Chem Soc* **2013**, *135* (33), 12164-12167.
- (53) Ferrauto, G.; Delli Castelli, D.; Di Gregorio, E.; Terreno, E.; Aime, S. LipoCEST and cellCEST imaging agents: opportunities and challenges. *Wiley Interdiscip Rev Nanomed Nanobiotechnol* **2016**, *8* (4), 602-618.
- (54) Abozeid, S. M.; Asik, D.; Sokolow, G. E.; Lovell, J. F.; Nazarenko, A. Y.; Morrow, J. R. Coll Complexes as Liposomal CEST Agents. *Angew Chem Int Ed* **2020**, *132* (29), 12191-12195.
- (55) Terreno, E.; Castelli, D. D.; Violante, E.; Sanders, H. M. H. F.; Sommerdijk, N. A. J. M.; Aime, S. Osmotically Shrunken LIPOCEST Agents: An Innovative Class of Magnetic Resonance Imaging Contrast Media Based on Chemical Exchange Saturation Transfer. *Chem-Eur J* **2009**, *15* (6), 1440-1448.
- (56) a) Delli Castelli, D.; Dastru, W.; Terreno, E.; Cittadino, E.; Mainini, F.; Torres, E.; Spadaro, M.; Aime, S. In vivo MRI multicontrast kinetic analysis of the uptake and intracellular trafficking of paramagnetically labeled liposomes. *J Control Release* **2010**, *144* (3), 271-279. b) Castelli, D. D.; Terreno, E.; Cabella, C.; Chaabane, L.; Lanzardo, S.; Tei, L.; Visigalli, M.; Aime, S. Evidence for in vivo macrophage mediated tumor uptake of paramagnetic/fluorescent liposomes. *Nmr Biomed* **2009**, *22* (10), 1084-1092.
- (57) Mulas, G.; Ferrauto, G.; Dastru, W.; Anedda, R.; Aime, S.; Terreno, E. Insights on the relaxation of liposomes encapsulating paramagnetic Ln-based complexes. *Magn Reson Med* **2015**, *74* (2), 468-473.
- (58) Kneepkens, E.; Fernandes, A.; Nicolay, K.; Grull, H. Iron(III)-Based Magnetic Resonance-Imageable Liposomal T1 Contrast Agent for Monitoring Temperature-Induced Image-Guided Drug Delivery. *Invest Radiol* **2016**, *51* (11), 735-745.

- (59) Langereis, S.; Geelen, T.; Grull, H.; Strijkers, G. J.; Nicolay, K. Paramagnetic liposomes for molecular MRI and MRI-guided drug deliveryc (vol 26, pg 728, 2013). *NMR Biomed* **2013**, *26* (9), 1195-1195.
- (60) Abozeid, S. M.; Chowdhury, M. S. I.; Asik, D.; Spernyak, J. A.; Morrow, J. R. Liposomal Fe(III) Macrocyclic Complexes with Hydroxypropyl Pendants as MRI Probes. *Acs Appl Bio Mater* **2021**, *4* (11), 7951-7960.
- (61) Mulas, G.; Rolla, G. A.; Geraldes, C. F. G. C.; Starmans, L. W. E.; Botta, M.; Terreno, E.; Tei, L. Mn(II)-Based Lipidic Nanovesicles as High-Efficiency MRI Probes (vol 3, pg 2401, 2020). *Acs Appl Bio Mater* **2020**, *3* (6), 3924-3924.
- (62) Sokolow, G. E.; Crawley, M. R.; Morphet, D. R.; Asik, D.; Spernyak, J. A.; McGray, A. J. R.; Cook, T. R.; Morrow, J. R. Metal-Organic Polyhedron with Four Fe(III) Centers Producing Enhanced T1 Magnetic Resonance Imaging Contrast in Tumors. *Inorg Chem* **2022**, *61* (5), 2603-2611.
- (63) Du, K.; Waters, E. A.; Harris, T. D. Ratiometric quantitation of redox status with a molecular Fe-2 magnetic resonance probe. *Chemical Science* **2017**, *8* (6), 4424-4430.
- (64) Thorarinsdottir, A. E.; Du, K.; Collins, J. H. P.; Harris, T. D. Ratiometric pH Imaging with a Co-2(II) MRI Probe via CEST Effects of Opposing pH Dependences. *J Am Chem Soc* **2017**, *139* (44), 15836-15847.
- (65) Rancan, G.; Castelli, D. D.; Aime, S. MRI CEST at 1 T With Large μ_{eff} Ln(III) Complexes Tm-HPDO3A: An Efficient MRI pH Reporter. *Magn. Res. Med.* **2016**, *75*, 329-336.
- (66) Harvey, P.; Blamire, A. M.; Wilson, J. I.; Finney, K. L. N. A.; Funk, A. M.; Senanayake, P. K.; Parker, D. Moving the goal posts: enhancing the sensitivity of PARASHIFT proton magnetic resonance imaging and spectroscopy. *Chemical Science* **2013**, *4* (11), 4251-4258.
- (67) Kras, E. A.; Abozeid, S. M.; Eduardo, W.; Spernyak, J. A.; Morrow, J. R. Comparison of phosphonate, hydroxypropyl and carboxylate pendants in Fe(III) macrocyclic complexes as MRI contrast agents. *J Inorg Biochem* **2021**, *225*, 111594.
- (68) Asik, D.; Smolinski, R.; Abozeid, S. M.; Mitchell, T. B.; Turowski, S. G.; Spernyak, J. A.; Morrow, J. R. Modulating the properties of Fe (III) macrocyclic MRI contrast agents by appending sulfonate or hydroxyl groups. *Molecules* **2020**, *25* (10), 2291.
- (69) Snodin, M. D.; Ould-Moussa, L.; Wallmann, U.; Lecomte, S.; Bachler, V.; Bill, E.; Hummel, H.; Weyhermuller, T.; Hildebrandt, P.; Wieghardt, K. The molecular and electronic structure of octahedral tris(phenolato)iron(III) complexes and their phenoxyl radical analogues: A Mossbauer and resonance Raman spectroscopic study. *Chem-Eur J* **1999**, *5* (9), 2554-2565.
- (70) Tsitovich, P. B.; Spernyak, J. A.; Morrow, J. R. A redox-activated MRI contrast agent that switches between paramagnetic and diamagnetic states. *Angew Chem Int Ed Engl* **2013**, *52* (52), 13997-14000.
- (71) Wieghardt, K.; Bossek, U.; Chaudhuri, P.; Herrmann, W.; Menke, B. C.; Weiss, J. 1,4,7-Triazacyclononane-N,N',N"-Triacetate (Tcta), a Hexadentate Ligand for Divalent and Trivalent Metal-lons Crystal-Structures of [Criii(Tcta)], [Feiii(Tcta)], and Na[Cuii(Tcta)].2nabr.8h2o. *Inorg Chem* **1982**, *21* (12), 4308-4314.
- (72) O'Neill, E. S.; Kolanowski, J. L.; Yin, G. H.; Broadhouse, K. M.; Grieve, S. M.; Renfrew, A. K.; Bonnitcha, P. D.; New, E. J. Reversible magnetogenic cobalt complexes. *Rsc Adv* **2016**, *6* (36), 30021-30027.
- (73) Dorazio, S. J.; Tsitovich, P. B.; Gardina, S. A.; Morrow, J. R. The reactivity of macrocyclic Fe(II) paraCEST MRI contrast agents towards biologically relevant anions, cations, oxygen or peroxide. *J Inorg Biochem* **2012**, *117*, 212-219.
- (74) Bond, C. Analyzing paraCEST and water interactions of Fe(II) and Co(II) macrocyclic complexes for MRI contrast. Ph. D. thesis, University at Buffalo, the State University of New York, Buffalo, NY, 2019.
- (75) Go, Y. M.; Jones, D. P. Redox theory of aging: implications for health and disease. *Clin Sci* **2017**, *131* (14), 1669-1688.

- (76) Chaiswing, L.; St Clair, W. H.; St Clair, D. K. Redox Paradox: A Novel Approach to Therapeutics-Resistant Cancer. *Antioxid Redox Sign* **2018**, *29* (13), 1237-1272.
- (77) Jones, D. P.; Sies, H. The Redox Code. Antioxid Redox Sign 2015, 23 (9), 734-746.
- (78) Koppenol, W. H.; Hider, R. H. Iron and redox cycling. Do's and don'ts. *Free Radical Bio Med* **2019**, 133, 3-10.
- (79) Sies, H.; Belousov, V. V.; Chandel, N. S.; Davies, M. J.; Jones, D. P.; Mann, G. E.; Murphy, M. P.; Yamamoto, M.; Winterbourn, C. Defining roles of specific reactive oxygen species (ROS) in cell biology and physiology. *Nat Rev Mol Cell Bio* **2022**.
- (80) Berndt, C.; Lillig, C. H.; Flohe, L. Redox regulation by glutathione needs enzymes. *Front Pharmacol* **2014**, *5*, 1-4.
- (81) Wittmann, C.; Chockley, P.; Singh, S. K.; Pase, L.; Lieschke, G. J.; Grabher, C. Hydrogen peroxide in inflammation: messenger, guide, and assassin. *Adv Hematol* **2012**, *2012*, 541471.
- (82) Love, N. R.; Chen, Y. Y.; Ishibashi, S.; Kritsiligkou, P.; Lea, R.; Koh, Y.; Gallop, J. L.; Dorey, K.; Amaya, E. Amputation-induced reactive oxygen species are required for successful Xenopus tadpole tail regeneration. *Nat Cell Biol* **2013**, *15* (2), 222-228.
- (83) Semenza, G. L. Hypoxia-Inducible Factors in Physiology and Medicine. Cell 2012, 148 (3), 399-408.
- (84) a) Nathan, C.; Cunningham-Bussel, A. Beyond oxidative stress: an immunologist's guide to reactive oxygen species. *Nat Rev Immunol* **2013**, *13* (5), 349-361. b) Fisher, A. B. Redox Signaling Across Cell Membranes. *Antioxid Redox Sign* **2009**, *11* (6), 1349-1356.
- (85) Forman, H. J.; Bernardo, A.; Davies, K. J. A. What is the concentration of hydrogen peroxide in blood and plasma? (vol 603, pg 48, 2016). *Arch Biochem Biophys* **2016**, *607*, 7-7.
- (86) Joyner, J. C.; Cowan, J. A. Targeted Cleavage of HIV RRE RNA by Rev-Coupled Transition Metal Chelates. *J Am Chem Soc* **2011**, *133* (25), 9912-9922.
- (87) Gale, E. M.; Jones, C. M.; Ramsay, I.; Farrar, C. T.; Caravan, P. A Janus Chelator Enables Biochemically Responsive MRI Contrast with Exceptional Dynamic Range. *J Am Chem Soc* **2016**, *138* (49), 15861-15864.
- (88) Khan, A. A.; Alsahli, M. A.; Rahmani, A. H. Myeloperoxidase as an Active Disease Biomarker: Recent Biochemical and Pathological Perspectives. *Med Sci (Basel)* **2018**, *6* (2).
- (89) Carreau, A.; El Hafny-Rahbi, B.; Matejuk, A.; Grillon, C.; Kieda, C. Why is the partial oxygen pressure of human tissues a crucial parameter? Small molecules and hypoxia. *J Cell Mol Med* **2011**, *15* (6), 1239-1253.
- (90) Erez, A.; DeBerardinis, R. J. Metabolic dysregulation in monogenic disorders and cancer finding method in madness. *Nat Rev Cancer* **2015**, *15* (7), 440-448. DOI: 10.1038/nrc3949. Fukumura, D.; Jain, R. K. Tumor microvasculature and microenvironment: Targets for anti-angiogenesis and normalization. *Microvasc Res* **2007**, *74* (2-3), 72-84.
- (91) Roussakis, E.; Li, Z. X.; Nichols, A. J.; Evans, C. L. Oxygen-Sensing Methods in Biomedicine from the Macroscale to the Microscale. *Angew Chem Int Edit* **2015**, *54* (29), 8340-8362.
- (92) Glenister, A.; Chen, C. K. J.; Paterson, D. J.; Renfrew, A. K.; Simone, M. I.; Hambley, T. W. Warburg Effect Targeting Co(III) Cytotoxin Chaperone Complexes. *J Med Chem* **2021**, *64* (5), 2678-2690.
- (93) Brue, C. R.; Dukes, M. W.; Masotti, M.; Holmgren, R.; Meade, T. J. Functional Disruption of Gli1-DNA Recognition via a Cobalt(III) Complex. *Chemmedchem* **2022**, *17*, e202200025.
- 10.1002/cmdc.202200025. Heffern, M. C.; Yamamoto, N.; Holbrook, R. J.; Eckermann, A. L.; Meade, T. J. Cobalt derivatives as promising therapeutic agents. *Curr Opin Chem Biol* **2013**, *17* (2), 189-196. (94) Xie, D.; Yu, M.; Kadakia, R. T.; Que, E. L. F-19 Magnetic Resonance Activity-Based Sensing Using Paramagnetic Metals. *Acc Chem Res* **2020**, *53* (1), 2-10.

- (95) O'Neill, E. S.; Kaur, A.; Bishop, D. P.; Shishmarev, D.; Kuchel, P. W.; Grieve, S. M.; Figtree, G. A.; Renfrew, A. K.; Bonnitcha, P. D.; New, E. J. Hypoxia-Responsive Cobalt Complexes in Tumor Spheroids: Laser Ablation Inductively Coupled Plasma Mass Spectrometry and Magnetic Resonance Imaging Studies. *Inorg Chem* **2017**, *56* (16), 9860-9868.
- (96) Chen, Q.; Liang, C.; Sun, X. Q.; Chen, J. W.; Yang, Z. J.; Zhao, H.; Feng, L. Z.; Liu, Z. H2O2-responsive liposomal nanoprobe for photoacoustic inflammation imaging and tumor theranostics via in vivo chromogenic assay. *P Natl Acad Sci USA* **2017**, *114* (21), 5343-5348.
- (97) a) Dorazio, S. J.; Tsitovich, P. B.; Siters, K. E.; Spernyak, J. A.; Morrow, J. R. Iron(II) PARACEST MRI Contrast Agents. *J Am Chem Soc* **2011**, *133* (36), 14154-14156. b) Olatunde, A. O.; Cox, J. M.; Daddario, M. D.; Spernyak, J. A.; Benedict, J. B.; Morrow, J. R. Seven-Coordinate Co-II, Fe-II and Six-Coordinate Ni-II Amide-Appended Macrocyclic Complexes as ParaCEST Agents in Biological Media. *Inorg Chem* **2014**, *53* (16), 8311-8321.
- (98) Tsitovich, P. B.; Gendron, F.; Nazarenko, A. Y.; Livesay, B. N.; Lopez, A. P.; Shores, M. P.; Autschbach, J.; Morrow, J. R. Low-Spin Fe(III) Macrocyclic Complexes of Imidazole-Appended 1,4,7-Triazacyclononane as Paramagnetic Probes. *Inorg Chem* **2018**, *57* (14), 8364-8374.
- (99) Tsitovich, P. B.; Kosswattaarachchi, A. M.; Crawley, M. R.; Tittiris, T. Y.; Cook, T. R.; Morrow, J. R. An Fe-III Azamacrocyclic Complex as a pH-Tunable Catholyte and Anolyte for Redox-Flow Battery Applications. *Chem-Eur J* **2017**, *23* (61), 15327-15331.
- (100) Snyder, E. M.; Asik, D.; Abozeid, S. M.; Burgio, A.; Bateman, G.; Turowski, S. G.; Spernyak, J. A.; Morrow, J. R. A Class of FeIII Macrocyclic Complexes with Alcohol Donor Groups as Effective T1 MRI Contrast Agents. *Angew Chem Int Ed* **2020**, *132* (6), 2435-2440.
- (101) Wang, H.; Cleary, M. B.; Lewis, L. C.; Bacon, J. W.; Caravan, P.; Shafaat, H. S.; Gale, E. M. Enzyme Control Over Ferric Iron Magnetostructural Properties. *Angew Chem Int Ed* **2022**, *61*, e202114019.
- (102) Ekanger, L. A.; Ali, M. M.; Allen, M. J. Oxidation-responsive Eu2+/3+- liposomal contrast agent for dual-mode magnetic resonance imaging. *Chem Commun* **2014**, *50* (94), 14835-14838.
- (103) Olatunde, A. O.; Dorazio, S. J.; Spernyak, J. A.; Morrow, J. R. The NiCEST Approach: Nickel(II) ParaCEST MRI Contrast Agents. *J Am Chem Soc* **2012**, *134* (45), 18503-18505.
- (104) a) Xie, D.; Ohman, L. E.; Que, E. L. Towards Ni(II) complexes with spin switches for F-19 MR-based pH sensing. *Magn Reson Mater Phy* **2019**, *32* (1), 89-96. b) Heitmann, G.; Schutt, C.; Grobner, J.; Huber, L.; Herges, R. Azoimidazole functionalized Ni-porphyrins for molecular spin switching and light responsive MRI contrast agents. c) *Dalton Trans* **2016**, *45* (28), 11407-11412. Heitmann, G.; Schutt, C.; Herges, R. Spin State Switching in Solution with an Azoimidazole-Functionalized Nickel(II)-Porphyrin. *Eur J Org Chem* **2016**, *2016* (22), 3817-3823.
- (105) Aime, S.; Botta, M.; Gianolio, E.; Terreno, E. A p(O-2)-responsive MRI contrast agent based on the redox switch of manganese(II/III) Porphyrin complexes. *Angew Chem Int Edit* **2000**, *39*, 746-750.
- (106) Gale, E. M.; Mukherjee, S.; Liu, C.; Loving, G. S.; Caravan, P. Structure–redox–relaxivity relationships for redox responsive manganese-based magnetic resonance imaging probes. *Inorg Chem* **2014**, *53* (19), 10748-10761.
- (107) Loving, G. S.; Mukherjee, S.; Caravan, P. Redox-Activated Manganese-Based MR Contrast Agent. *J Am Chem Soc* **2013**, *135* (12), 4620-4623.
- (108) Barandov, A.; Ghosh, S.; Li, N.; Bartelle, B. B.; Daher, J. I.; Pegis, M. L.; Collins, H.; Jasanoff, A. Molecular Magnetic Resonance Imaging of Nitric Oxide in Biological Systems. *Acs Sensors* **2020**, *5* (6), 1674-1682.
- (109) Dunbar, L.; Sowden, R. J.; Trotter, K. D.; Taylor, M. K.; Smith, D.; Kennedy, A. R.; Reglinski, J.; Spickett, C. M. Copper complexes as a source of redox active MRI contrast agents. *Biometals* **2015**, *28* (5), 903-912.
- (110) a) Xie, D.; Kim, S.; Kohli, V.; Banerjee, A.; Yu, M.; Enriquez, J. S.; Luci, J. J.; Que, E. L. Hypoxia-Responsive F-19 MRI Probes with Improved Redox Properties and Biocompatibility. *Inorg Chem* **2017**,

- 56 (11), 6429-6437. b) Xie, D.; King, T. L.; Banerjee, A.; Kohli, V.; Que, E. L. Exploiting Copper Redox for F-19 Magnetic Resonance-Based Detection of Cellular Hypoxia. *J Am Chem Soc* **2016**, *138* (9), 2937-2940. . (111) Du, K.; Harris, T. D. A Cu-2(II) Paramagnetic Chemical Exchange Saturation Transfer Contrast Agent Enabled by Magnetic Exchange Coupling. *J Am Chem Soc* **2016**, *138* (25), 7804-7807.
- (112) a) Catanzaro, V.; Gringeri, C. V.; Menchise, V.; Padovan, S.; Boffa, C.; Dastru, W.; Chaabane, L.; Digilio, G.; Aime, S. A R2p/R1p Ratiometric Procedure to Assess Matrix Metalloproteinase-2 Activity by Magnetic Resonance Imaging. *Angew Chem Int Edit* **2013**, *52* (14), 3926-3930. b) Aime, S.; Fedeli, F.; Sanino, A.; Terreno, E. A R-2/R-1 ratiometric procedure for a concentration-independent, pH-responsive, Gd(III)-based MRI agent. *J Am Chem Soc* **2006**, *128* (35), 11326-11327.
- (113) Peterson, K. L.; Srivastava, K.; Pierre, V. C. Fluorinated Paramagnetic Complexes: Sensitive and Responsive Probes for Magnetic Resonance Spectroscopy and Imaging. *Front Chem* **2018**, *6*. DOI: ARTN 160 10.3389/fchem.2018.00160.
- (114) Ratnakar, S. J.; Soesbe, T. C.; Lumata, L. L.; Do, Q. N.; Viswanathan, S.; Lin, C. Y.; Sherry, A. D.; Kovacs, Z. Modulation of CEST Images in Vivo by T-1 Relaxation: A New Approach in the Design of Responsive PARACEST Agents. *J Am Chem Soc* **2013**, *135* (40), 14904-14907.
- (115) Manea, S. A.; Vlad, M. L.; Rebleanu, D.; Lazar, A. G.; Fenyo, I. M.; Calin, M.; Simionescu, M.; Manea, A. Detection of Vascular Reactive Oxygen Species in Experimental Atherosclerosis by High-Resolution Near-Infrared Fluorescence Imaging Using VCAM-1-Targeted Liposomes Entrapping a Fluorogenic Redox-Sensitive Probe. *Oxid Med Cell Longev* **2021**, *2021*. DOI: Artn 6685612, 10.1155/2021/6685612.
- (116) Wang, C. H.; Cheng, D.; Motlagh, N. J.; Kuellenberg, E. G.; Wojtkiewicz, G. R.; Schmidt, S. P.; Stocker, R.; Chen, J. W. Highly Efficient Activatable MRI Probe to Sense Myeloperoxidase Activity. *J Med Chem* **2021**, *64* (9), 5874-5885.
- (117) Wu, J. The Enhanced Permeability and Retention (EPR) Effect: The Significance of the Concept and Methods to Enhance Its Application. *J Pers Med* **2021**, *11*, 771.
- 10.3390/jpm11080771. Shi, Y.; Van der Meel, R.; Chen, X. Y.; Lammers, T. The EPR effect and beyond: Strategies to improve tumor targeting and cancer nanomedicine treatment efficacy. *Theranostics* **2020**, *10* (17), 7921-7924.
- (118) Waghorn, P. A.; Jones, C. M.; Rotile, N. J.; Koerner, S. K.; Ferreira, D. S.; Chen, H. H.; Probst, C. K.; Tager, A. M.; Caravan, P. Molecular Magnetic Resonance Imaging of Lung Fibrogenesis with an Oxyamine-Based Probe. *Angew Chem Int Edit* **2017**, *56* (33), 9825-9828. Akam, E. A.; Abston, E.; Rotile, N. J.; Slattery, H. R.; Zhou, I. Y.; Lanuti, M.; Caravan, P. Improving the reactivity of hydrazine-bearing MRI probes for in vivo imaging of lung fibrogenesis. *Chem Sci* **2020**, *11* (1), 224-231.